JOURNAL OF MATERIALS SCIENCE 20 (1985) 2045–2059

Fatigue behaviour of synthetic fibres, yarns, and ropes

M. C. KENNEY*, J. F. MANDELL, F. J. McGARRY
Department of Materials Science and Engineering, Massachusetts Institute of Technology, Cambridge, Massachusetts 02139, USA

S–N fatigue and creep-rupture data have been obtained for nylon 6,6 single fibres, interlaced yarns, and small ropes under a variety of loading conditions. The results show a similar degradation rate at each level of structure, with no apparent influence of inter-fibre effects. Cyclic lifetimes of single fibres of nylon 6,6 as well as polyester and aramid can be predicted from a creep rupture model. Consistent with this model, the time to failure is insensitive to frequency over a broad range. For each level of structure the strain at failure is the same whether tested in simple tension or under cyclic or creep loading. Failure modes were generally similar in creep rupture and cyclic fatigue tests; no effect of a slack load on each cycle was evident either in the failure mode or specimen lifetime.

1. Introduction

Oriented fibre structures are used in many applications where a combination of good axial mechanical properties and light weight is required. The use of nylon fibres and yarns in marine ropes is one application which has grown considerably over the past 15 years. As with many applications, marine ropes in service are subjected to a complex history of static and cyclic mechanical loading [1], which may, in some cases, end in sudden and unexpected failure. This work is concerned with determining the mechanisms by which cyclic fatigue loading causes failure in oriented fibre structures, with emphasis on nylon single fibre and yarn properties, and additional work on small rope structures and other materials.

The effects of fatigue loading in polymers as a general class of materials is receiving increasing attention in the current literature (a recent review is given in [2]). In bulk polymers, failure during cycling can occur by a number of modes [3]. Some polymers such as nylon, with large hysteresis loops and poor thermal conductivity, may fail thermally as a result of internal hysteretic heating. The material may also respond to cycling as if a static load had been applied continuously for an equivalent period of time, with failures occurring at times and elongations similar to creep loading [4, 5]. Finally, failure in bulk polymers may occur as a result of fatigue crack initiation and stable propagation, similar to that in metals. For nylon in fibrous form, some evidence exists for all three modes [6–8].

2. Experimental procedure

Fatigue testing was conducted using closed loop servohydraulic machines. Most tests were run in the load control mode, using a sine wave function. Ultimate tensile load was evaluated using a ramp test (constant loading rate) to failure at a rate equivalent to the averaged loading portion of the fatigue cycle. Fatigue testing was conducted to various percentages of this ultimate tensile load. The specimens were cycled between the maximum load and one-tenth of this value; i.e. the ratio $\sigma_{min}/\sigma_{max}$ (or stress ratio, R) was equal to 0.1. (Other R values have been used in some cases.) For single fibre fatigue testing, a specially designed steel beam support frame on pneumatic shock absorbers was constructed to minimize vibrations transmitted from the hydraulics and floor. A 2000 g capacity load cell suspended from this

*Present address: Albany International Research Co, Dedham, MA 02026, USA.

0022–2461/85 $03.00 + .12

frame registers approximately 1.5 g noise. The number of cycles to failure was recorded for each specimen. Various parameters, such as load, displacement and hysteresis energy were monitored using a minicomputer.

A master frequency of 1 Hz was used for most testing, master frequency referring to the frequency corresponding to cycling at 100% of ultimate tensile load. The actual test frequency at each percentage of ultimate tensile load was then adjusted upward to maintain a constant average loading rate. Thus, the frequency was increased as the maximum load was decreased. Test frequency was kept as close as possible to this level, except where machine resonances required slightly lower values. The master frequency is given on each figure.

A cardboard tabbing system was used for testing of yarns and single fibres. A flexible silicone sealant was incorporated at the tab end to improve stress transfer, and protect the specimen from abrasion. Further into the tab the specimen was bonded with a rigid adhesive (Eastman 910). Using this tabbing method, the majority of fibre breaks occurred in the gauge section, away from the grips, and were considered valid test results. For rope gripping, silicone and polyester adhesives were used to encapsulate rope ends into tapered metal fittings. The gauge length between rigid adhesive points for single fibres and yarns was 5 in (127 mm); the gauge length between fittings for small ropes was 4 in. (102 mm).

Dead load creep rupture lifetimes for fibres and yarns were also measured using tabbed specimens. The top of the specimen was hung from a support and weights were suspended from the bottom. Selected creep rupture tests were also run on the servohydraulic machines to allow better monitoring of data; failure times in these tests agreed well with dead load data.

The primary material was DuPont 707 nylon 6,6 yarn, a standard rope yarn used commercially. The yarn consists of 210 lightly interlaced fibres producing a total of 1260 denier, taken from a single lot and merge; the single fibre diameter was 30 μm. The small rope was a 3/16 in diameter double braided based on DuPont 707 nylon yarn, purchased from Sampson Ocean Systems. Except for single fibre creep rupture tests which were run at 65% RH, the humidity was not controlled. However, yarn creep rupture lifetimes obtained throughout the year were indistinguishable from those at 65% RH.

3. Results and discussion

3.1. Fibre, yarn, and small rope fatigue

Single fibre and yarn S–N data are plotted in Fig. 1. The fatigue data are presented as normalized

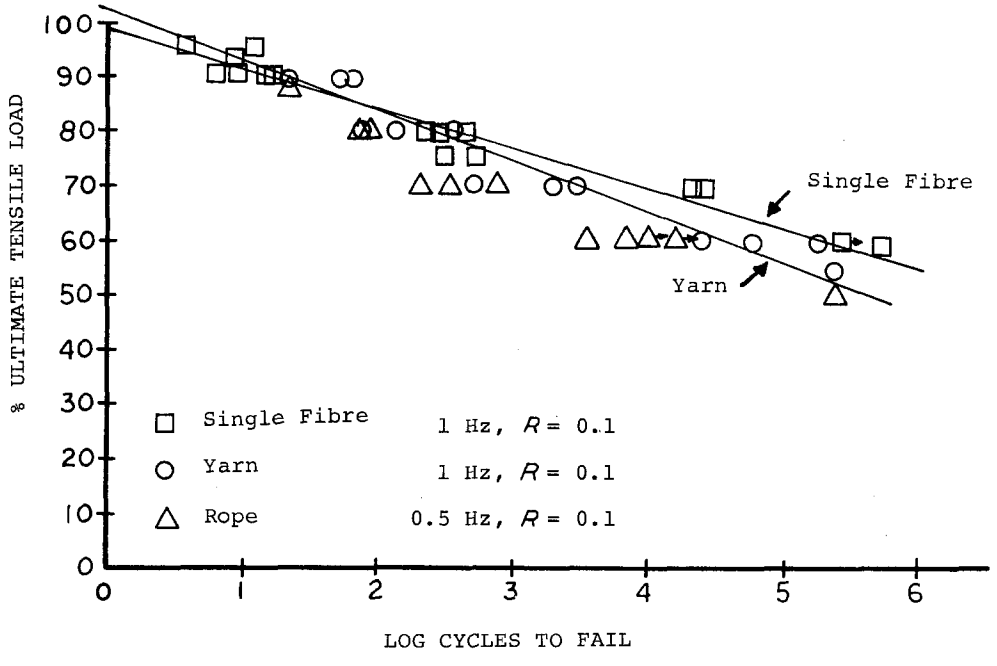

Figure 1 S–N fatigue data for DuPont 707 nylon single fibres, yarns, and 3/16 in. double braided rope.

TABLE I Ultimate load and elongation in single cycle ramp tests

	Ultimate* load	Ultimate* stress (MPa)	Ultimate* elongation (%)
Fibre	68.1 g (± 2.0)	965	15.0 (± 0.75)
Yarn	11.61 kg (± .43)	779	17.0 (± 1.4)
Rope	605 kg (± 21)		40.9 (± 2.0)

*Approximate failure time = 0.5 sec.

plots based on the single cycle ultimate tensile load for the conditions of that particular data set. Table I gives values of ultimate tensile load at failure for the specimens tested; these can be used to determine absolute load values for the S–N data. The lines on the graph show least square regressions of experimental data (not including single cycle ramp tests). Both sets of data are approximately linear, and show a steady decrease in lifetime with increasing maximum load. The linearity of these data and absence of a break in the curve imply that a single mechanism may operate throughout the fatigue range studied. These S–N curves are consistent with literature data [9–11]. For example, at about 60% of ultimate load, lifetimes are approximately 10^5 cycles.

It is important to note that the normalized graphs of the single fibre and yarn nearly superimpose. This can be seen from Fig. 1, or by comparing the regression equations, with 95% confidence limits given in parentheses:

$$\text{single fibre: } P/P_{ult} = 1.00\,(\pm 0.04) - 0.077\,(\pm 0.002)\log N$$

$$\text{yarn: } P/P_{ult} = 1.02\,(\pm 0.04) - 0.09\,(\pm 0.003)\log N$$

where P is the load and N is cycles to failure. Thus, the two levels of structure show essentially the same fatigue resistance. This implies a common factor in the fatigue degradation of each, which does not appear sensitive to structural or interfibre effects at this level.

Fatigue data for the small ropes are also given in Fig. 1. Tests were conducted at a frequency of 0.5 Hz. A fan was used to cool the rope during cycling to reduce the hysteretic temperature rise, which was otherwise substantial. Failure in the grips became a problem at lower loads and longer times. Grip failure points are indicated by arrows in Fig. 1 and represent the lowest possible gauge section lifetimes; gauge section failure could have occurred at longer times. The rope data points fall close to those of both the single fibre and yarn. Even if a slight adjustment were made for differences in frequency, the points would fall at similar times, indicating that interfibre contact and other structural differences have a minimal effect in the small rope as well as in the yarn.

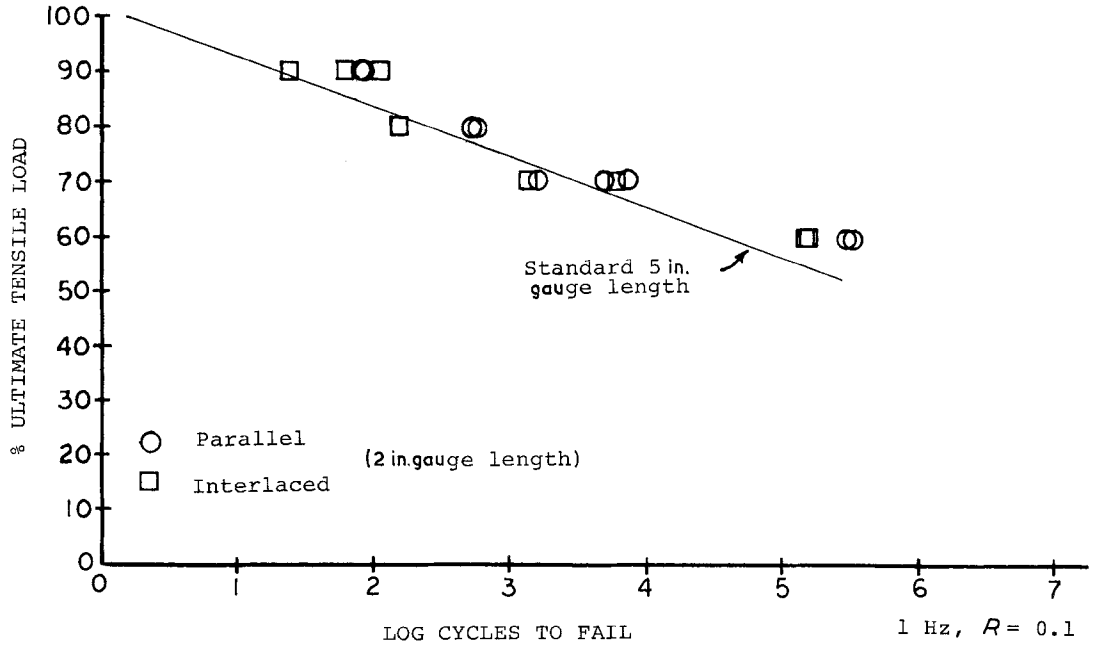

Figure 2 S–N fatigue data for parallel and interlaced sections of nylon yarn.

To further investigate possible interfibre or structural effects several studies were conducted, including interlaced and parallel yarn sections, added lubricants, and specimens composed of three contacting fibres. The DuPont 707 yarn is lightly interlaced by a jet of air blown orthogonally at the yarn during production, resulting in a lightly entangled point every 2 in on average, so all standard 5 in yarn specimens probably contained at least one interlace. To investigate this effect, short sections of yarn (2 in) were prepared containing either an interlaced point or a completely parallel length. A standard fatigue S–N curve was determined for each (Fig. 2). Fatigue data are identical for the parallel and interlaced specimens, as well as for specimens of standard length. Apparently, the interlace has no significant effect on fatigue performance.

The effect of a lubricant on dry yarn performance was examined briefly using a silicone fibre finish, Union Carbide LE-9300, applied as an emulsion and catalysed for full cure. A limited number of yarn fatigue tests at one load were conducted, and showed that the lubricant had no significant effect on the cycles to failure. A few tests were also run after the application of a standard silicone lubricating spray, and again no effect was found. This is not surprising in view of the absence of interfibre effects already demonstrated.

In a final study of interfibre effects, specimens were prepared with three fibres twisted together (two turns per inch). Fatigue data for these are compared to normalized single fibre lifetimes in Fig. 3. Lifetimes for specimens with three fibres in contact are clearly comparable to those for single fibres at this low twist level.

All of the data reported in this section indicate that the single fibre fatigue behaviour determines the yarn and, apparently, small rope fatigue behaviour without any significant complications. While the average single fibre tensile strength is not completely realized in the average yarn strength, due to long recognized statistical bundle effects [12], the rate of loss of the initial tensile strength in fatigue (slope of the normalized S–N curve) is similar for all three structures. Interlace regions and added lubricants do not affect yarn fatigue. However, in highly twisted yarns and in larger rope structures with more lateral pressure and relative movement, interfibre interactions and lubricant performance could become important.

3.2. Frequency effects

As interfibre effects at the yarn level have no significant effect on fatigue performance under the

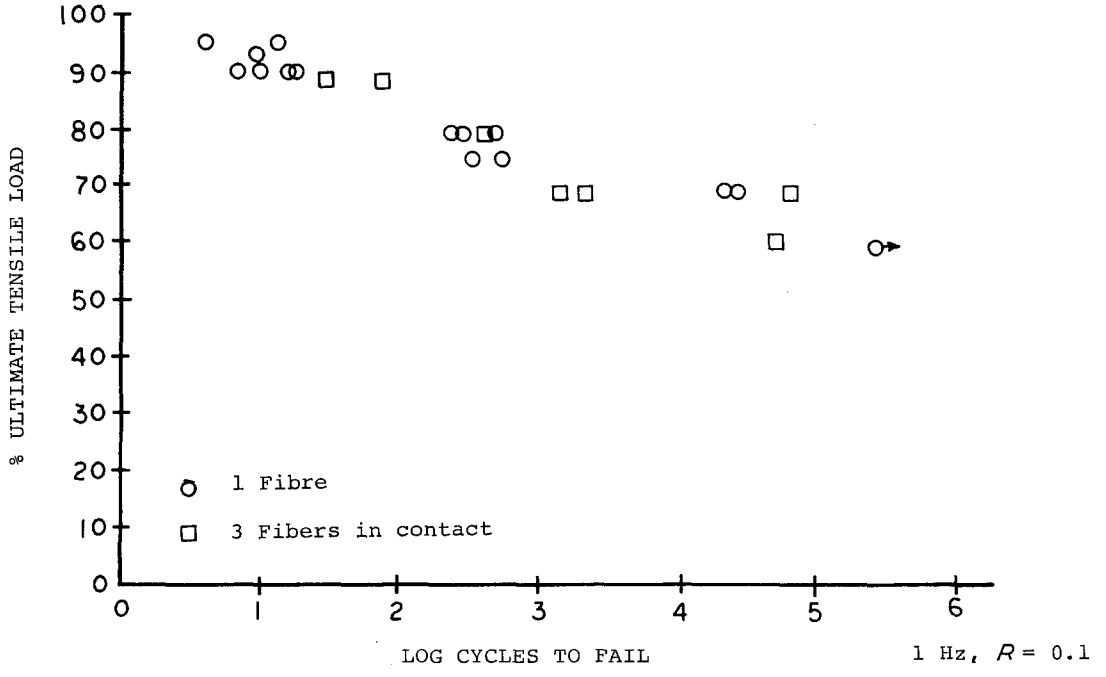

Figure 3 S–N fatigue data for single nylon fibres and for three fibres in contact.

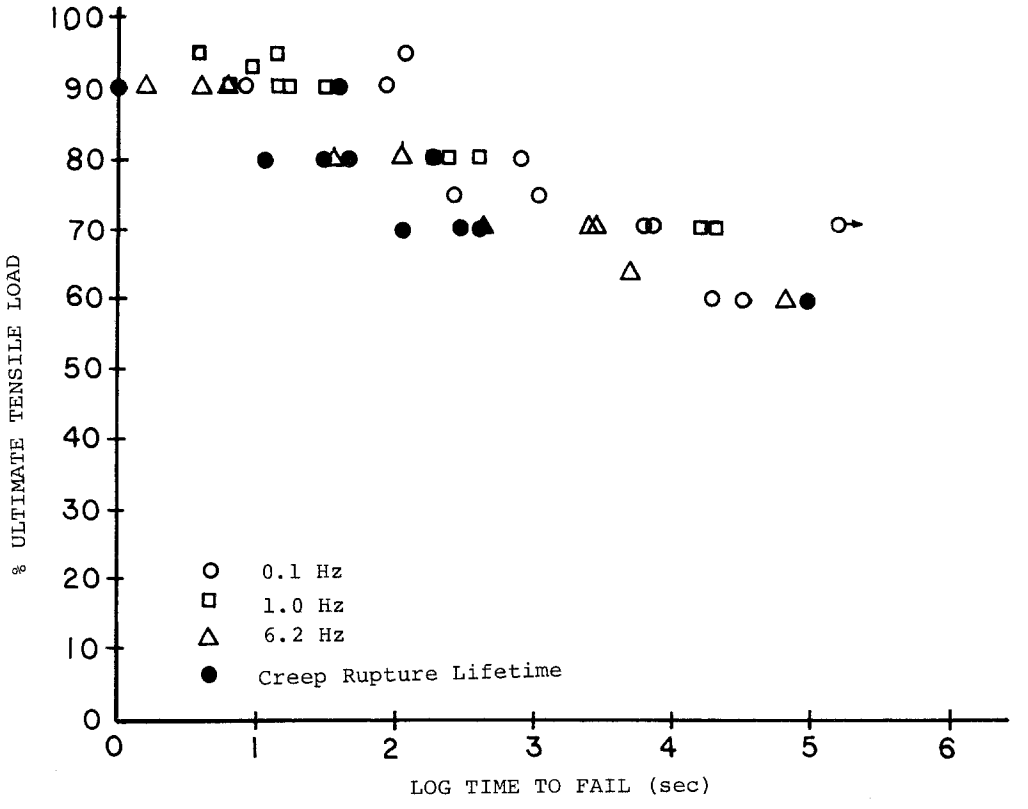

Figure 4 Fatigue data for single nylon fibres at several frequencies, plotted against total test time for comparison with creep rupture data.

conditions studied, the controlling mechanism must, therefore, be the individual response of the fibres to the applied loading. The failure mode under the applied loading may be dominated either by creep rupture (depending on time under load), traditional fatigue crack initiation and growth (depending on the number of cycles [3]), or hysteretic heating and the associated temperature rise. The dominance of a particular effect may be determined by varying the fatigue loading parameters and frequency.

Fig. 4 gives fatigue data for single fibres tested at frequencies of 0.1, 1.0, and 6.2 Hz. The 0.1 and 1.0 Hz tests were conducted in the usual manner with the frequency adjusted upward to maintain constant loading rate. The 6.2 Hz tests, however, could not be adjusted upward because of machine resonances, and were run at a constant frequency; this should have little effect over this broad range of frequencies. Note that the data are plotted as a function of log time to fail, rather than cycles to fail. The total test lifetime is equivalent regardless of test frequency, and is also similar to constant force, creep rupture data also shown in Fig. 4. These data indicate that single fibres fail according to a total time under load criterion.

Corresponding fatigue data for yarns tested at frequencies of 0.1, 1.0 and 10 Hz are given in Fig. 5. (Again, adjustment could not be made exactly for the 10 Hz tests because of machine resonance and performance limits.) Temperature change from hysteretic heating was monitored for the highest test frequency using a temperature sensitive lacquer (Omega Lac 100). No colour-change was observed in the lacquer, indicating that the temperature did not exceed 100° F. This is consistent with the literature [7] and shows that complications of a thermal failure mode are not present. An intensive series of tests was also run on yarns at these frequencies at two specific load levels (80% and 60% of the 1 Hz ramp strength). Specimens were prepared identically and tested in random order. Time and cycles to fail for these individual specimens are given in Table II. Both sets of data show that yarns follow a time under load criterion, as do the single fibres. Within the range of experimental scatter, the time to fail is constant regardless of the frequency of testing

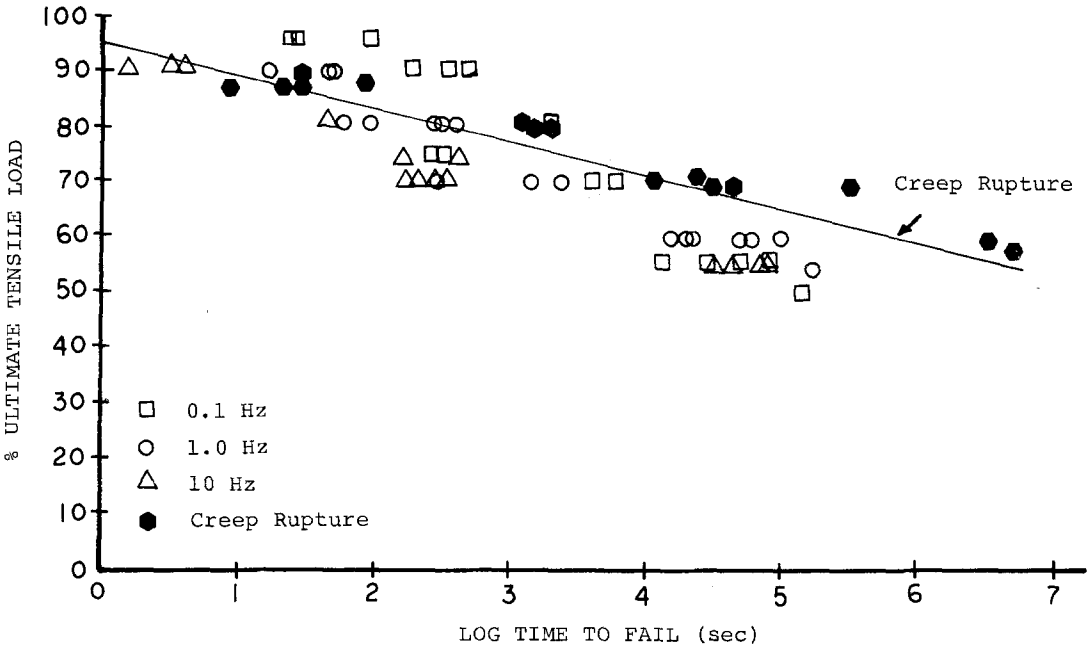

Figure 5 Fatigue data for nylon yarns at several frequencies compared with creep rupture data.

TABLE II Fatigue lifetime of yarn at various frequencies (single specimen data)

Frequency (Hz)	Log (cycles to fail)	Log (time to fail, sec)	Total elongation (%)
80% ultimate load*			
0.167	1.690	2.467	16.7
	1.716	2.493	16.3
1.67	2.846	2.624	> 16.3
	2.723	2.501	17.8
10	3.223	2.223	16.3
	3.625	2.625	18.7
60% ultimate load*			
0.167	3.897	4.674	17.1
	3.312	4.089	18.4
	4.152	4.930	15.4
	3.685	4.462	17.5
1.67	4.983	4.760	17.4
	4.527	4.305	17.5
	4.522	4.300	17.6
10	5.868	4.868	17.6
	5.810	4.810	–
	5.649	4.649	17.5
	5.549	4.549	17.0

*As measured in a 1 Hz test.

over the three frequencies used in this study (0.1, 1.0, 10 Hz). The common time under load failure dependence of both fibres and yarns is consistent with the equivalent S–N behaviour observed at 1 Hz. This type of frequency dependence contrasts with that found in the literature for bulk nylon where crack growth rate per cycle, rather than total test time, remains similar as frequency is changed [3]. The observed contrast in behaviour may result either from the dimensional characteristics or oriented structure of the fibres, or from material differences. Studies on acrylic and nylon fibres [6, 13] have shown decreasing time to fail with increasing frequency, but the extremely high frequencies used (50 to 90 Hz) could have affected these results.

3.3. Failure strain

Table III gives failure strains for single fibres, yarns, and small ropes for various types of loading. Under all loading conditions studied (fatigue, creep, and single cycle ramp tests) the total cumulative strain reached at failure is roughly constant for a given level of structure. The overall strain reached is, of course, influenced by the structure; it increases from fibre to rope as the structure becomes more geometrically complex. Similar

TABLE III Comparison of single cycle ramp, fatigue, and creep values of failure strain

	Failure strain (%)		
	Ramp	Fatigue*	Creep*
Fibre	15.0 (± 0.75)	14.6	14.4
Yarn	17.0 (± 1.4)	18.9	18.9
Rope	40.9 (± 2.0)	41.9	41.4

*Single specimen at 70% ultimate load, typical data.

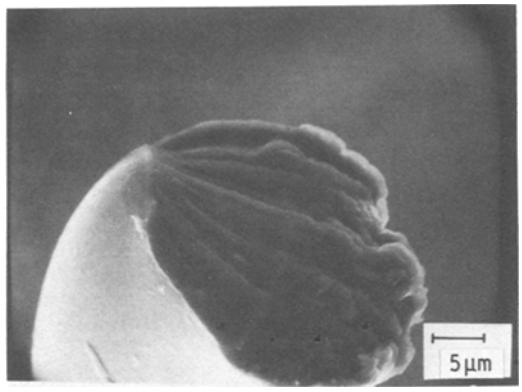

Figure 7 Fracture surface of nylon fibre failed in fatigue at 90% of ultimate load.

failure strains are also reached regardless of test frequency, as is shown for yarns in Table II. Fig. 6 shows that the strain accumulating with total test time is remarkably insensitive to the frequency or number of cycles. Just prior to failure the strain increases rapidly as some fibres fail. Tests with a combination of loading conditions, as in tests where cycling is followed by ramp testing, also show a constant cumulative failure strain equivalent to the initial ramp value.

The observation that failure occurs at a particular strain for any level of structure, for all loading conditions, provides further strong support for the dominance of simple creep rupture in controlling failure. The creep behaviour of the single fibre, as moderated by increasing structural complexity, may determine the limiting extension in each level of structure studied. Within the single fibre, on a molecular level, this could be interpreted from various nylon models as either the accumulation of a critical number of taut tie molecules in the amorphous region [14], or as reaching a limiting extension of the oriented interfibrillar regions [15].

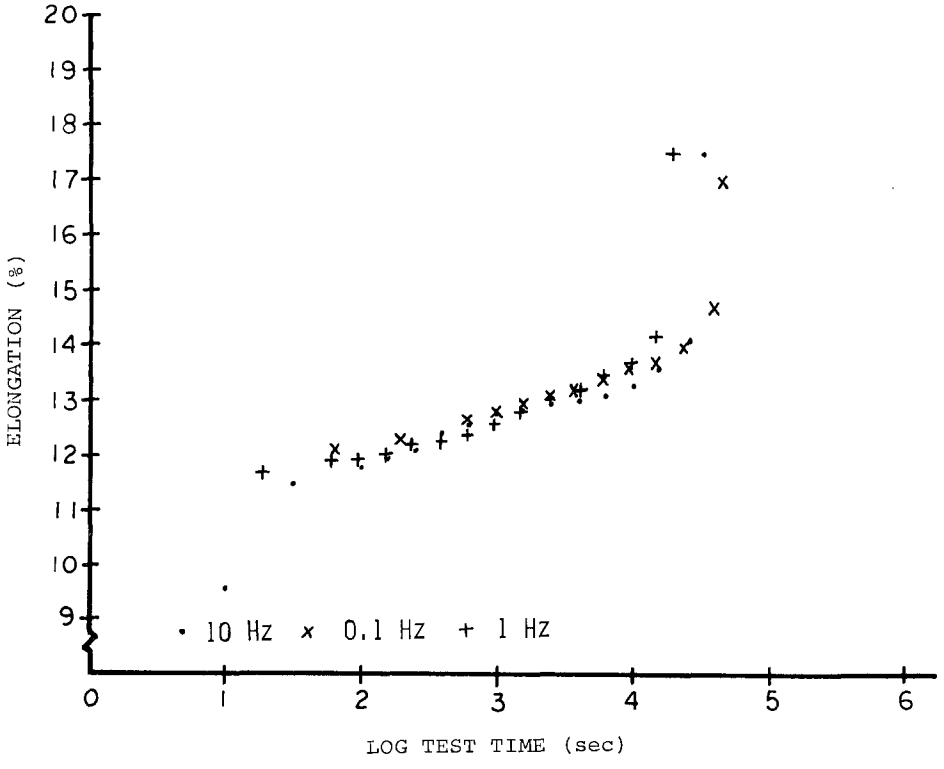

Figure 6 Elongation during fatigue for nylon yarns at three frequencies, tested at 60% of ultimate load.

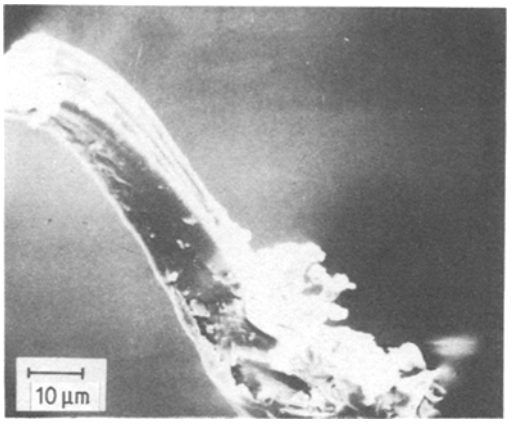

Figure 8 Fracture surface of fibre from nylon yarn failed in fatigue at 50% of ultimate load.

3.4. Fractographic study

Two types of fracture surfaces were observed in this study which are generally similar to those reported in the literature [6]. Fig. 7 shows the most typical surface, the classic scallop shell transverse fracture observed in many textile fibres. In this fracture, a crack initiates at the surface, then grows generally transverse to the fibre axis through a slow growth region. Finally, there is a fairly sharp transition to the fast fracture region. Fig. 8 shows a second type of fracture which also appears to initiate at the surface, but then is dominated by splitting generally parallel to the fibre axis, in a mode described as fibrillated [6].

Transverse failures were observed for all fatigue breaks at high loads and for most fatigue breaks at low loads. In approximately 5% of breaks at low loads in yarns a fibrillated fracture was observed. This behaviour is not unique to fatigue breaks, as both types of fractures were also observed for specimens from creep rupture tests at similar loads. This finding is contrary to reports in the literature [6] that in similar fibres the axial cracking mode is indicative of a unique fatigue failure mode and requires a slack load condition, which has been suggested to reduce fatigue lifetimes. The origin of this difference could be the higher frequency (50 Hz) used in the tests in Bunsell and Hearle [6], which could not be duplicated here.

Several fatigue tests were conducted on yarns using a slack loading condition ($R = 0$) at 1 Hz. The data shown in Fig. 9 fall within the previously determined fatigue lifetime scatter. Apparently, a period of slack load has no effect on yarn fatigue behaviour under these conditions, compared with tests at the usual $R = 0.1$.

Slack load fatigue tests were also run on single fibres, but at a frequency of 20 Hz. Because of dynamic (recording) effects, the measured load peak values were adjusted downward by 10% to give a better estimate of the actual loading. The

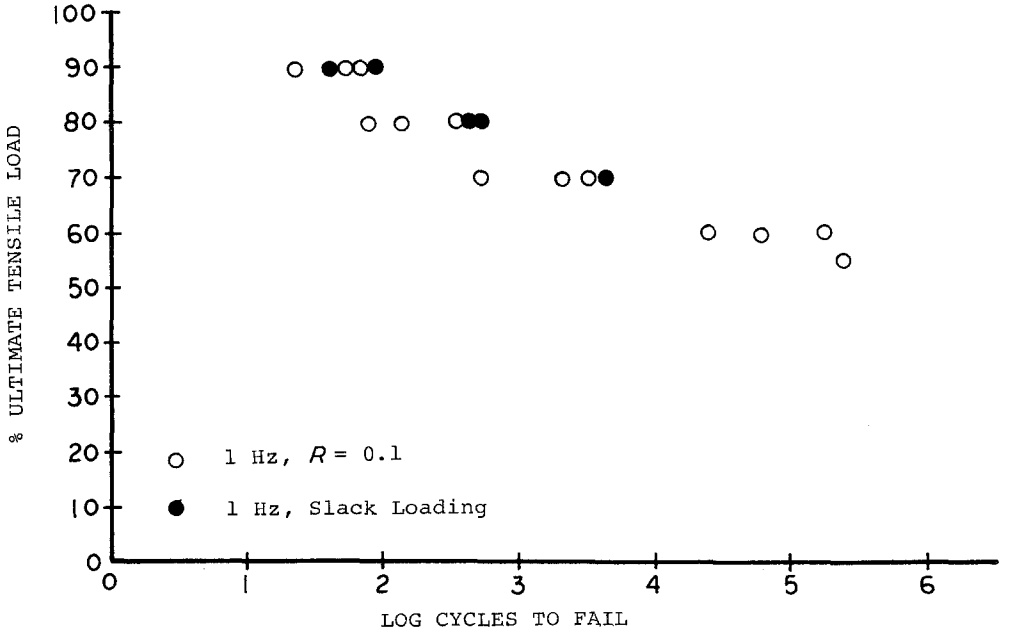

Figure 9 Effect of slack condition during each cycle in fatigue of nylon yarns.

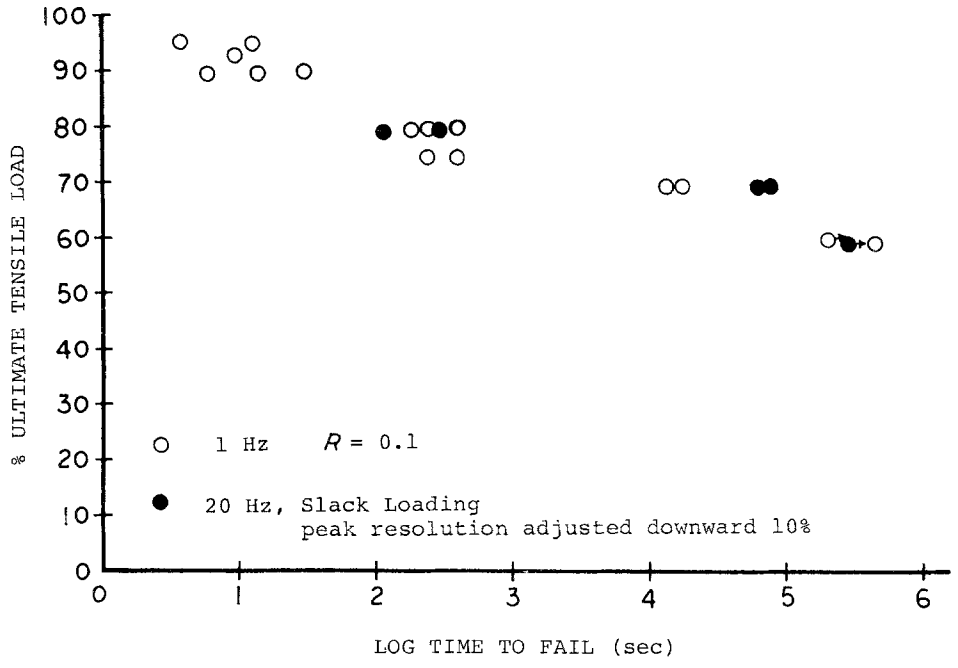

Figure 10 Effect of slack condition at high frequency on single nylon fibres.

adjusted data are plotted in Fig. 10, along with the fatigue data at 1 Hz. Two features are apparent: the high frequency data follow quite closely the fatigue behaviour at 1 Hz, and the presence of a slack load does not reduce the fatigue lifetime below the expected range. Fibre fracture surfaces from these tests also show a mixture of transverse and axial types. Our data, including observation of the axial mode in creep as well as cyclic tests, suggest that the axial splits do not require cyclic or slack loads, and that the mode of cracking does not influence the lifetime over the frequency range studied here. The occurrence of axial cracking clearly reflects the longitudinal structure of nylon with some preferred path between fibril or microfibril units. Kevlar fibres, with a more nearly perfect orientation, were observed to fail in the axial mode under all loading conditions in this study. Failures of the type described here suggest a fatigue crack growth controlled failure. In bulk polymers this would usually suggest a cyclic, rather than creep, dominated behaviour which could be considered in a fracture mechanics context. However, previous results for the strains at failure, and the similar times to fail under differing conditions are more consistent with a creep rupture mode. While cracks are clearly associated with eventual failure of the fibres, they may not represent the typical fatigue cracks which dominate bulk polymer breakdown [3], but rather represent a limiting rearrangement and extension of the fibre structure which is a consequence of creep.

3.5. Residual strength

Residual strength tests were conducted at various fractions of specimen lifetimes, typically 25, 50, and 75% of the mean lifetime, at a variety of load levels. Residual strength was determined within approximately 1 min of the end of cycling. The single fibre data in Fig. 11 show that the residual strength is almost equal to the original ultimate strength under all conditions. Thus, failure must occur in a sudden death fashion, with little decrease in strength before the fibre fails. The residual strain to failure shows a more gradual decrease as creep occurs. For a single fibre tested at 80% of the UTS for 75% of its lifetime, the residual strain to failure is approximately 75% of the initial value.

Higher levels of structure show somewhat more gradual property changes due to structural rearrangements and single fibre failures. For example, a yarn tested at 70% of its UTS contained almost exactly 70% of the original fibres unbroken just prior to failure. Thus, strength degradation in yarns and small ropes may be explained more by accumulating broken fibres than by changes in unbroken fibres. Permanent strains accumulating

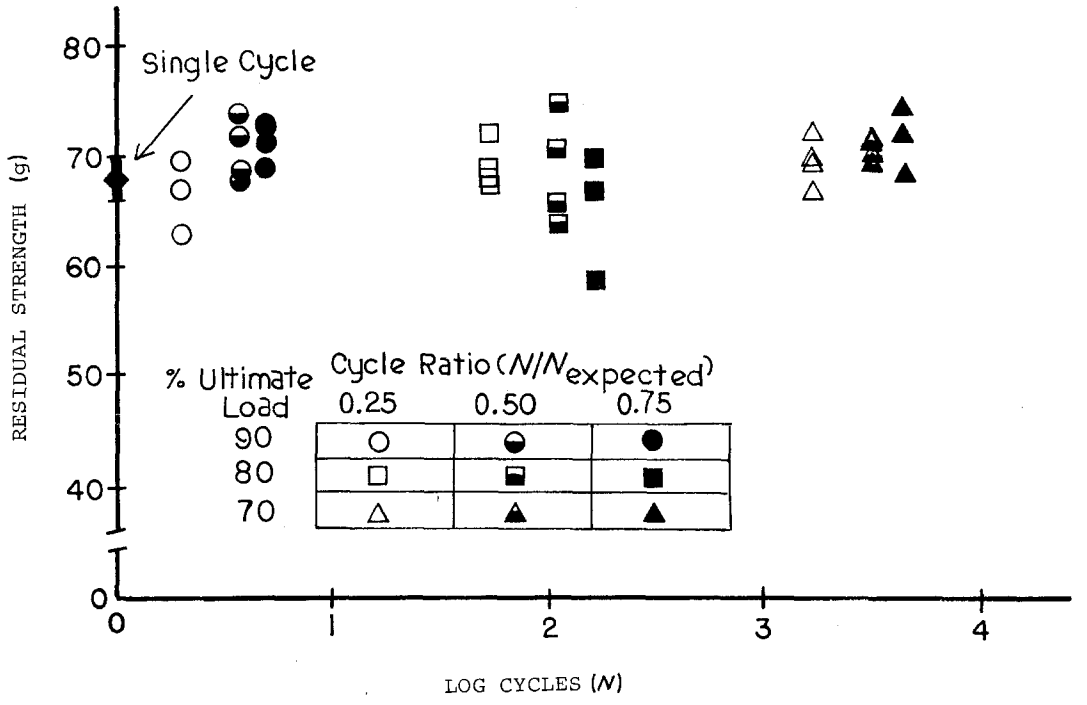

Figure 11 Residual strength of single nylon fibres after fatiguing various fractions of their lifetimes at three load levels.

during fatigue are also greater with yarns and ropes. A small rope tested at 60% of its UTS for 75% of its lifetime has a permanent creep strain of approximately 60% of its original failure strain.

3.6. Creep rupture model for fatigue life

Evidence for a simple creep rupture mechanism controlling failure in single fibres, yarns and small ropes appears quite strong. Normalized S–N curves are similar for all three structures. Interfibre effects are minimal in these yarns and small ropes, and do not appear to influence failure. Time to fail at the same load remains constant over a range of frequencies for both single fibres and yarns. Also, a constant strain is reached at failure, for a given structure, regardless of loading pattern or frequency. All of these results point strongly to a simple creep rupture mechanism. The constant failure strain [16] and time to failure regardless of frequency [17] have been reported in earlier fibre studies under more restrictive loading conditions.

A creep rupture failure mechanism may be analysed using the concepts of reaction rate theory and accumulation of damage [5]. This approach has been applied in the literature to both fibres and bulk materials [4, 5]. According to one typical approach [4], failure is approximated by dividing the sinusoidal fatigue wave into many small increments and weighting each increment by its failure time under pure creep loading; when the fractional lifetimes sum to 1, failure occurs. (This criterion is analogous to Miner's rule used in cycle dominated cases.) Failure then may be expressed as:

$$\int_0^{t_b} \frac{d(t)}{\tau_b \sigma(t)} \tag{1}$$

where τ_b is the time to fail under constant stress (creep rupture), σ is the applied stress, and t_b is the time to fail under sinusoidal stress.

Creep rupture is expressed in the form:

$$\tau_b = A \exp^{-B\sigma} \tag{2}$$

where A and B are experimentally measured constants. The creep rupture data which have been collected for single fibres, yarns, and small ropes all follow this type of relationship. For the case of sinusoidally varying load, the appropriate expression for σ is:

$$\sigma(t) = P + Q \sin(\omega t). \tag{3}$$

When these expressions are substituted into Equation 1 the integral may be solved using a zero order modified Bessel function giving the time to break as:

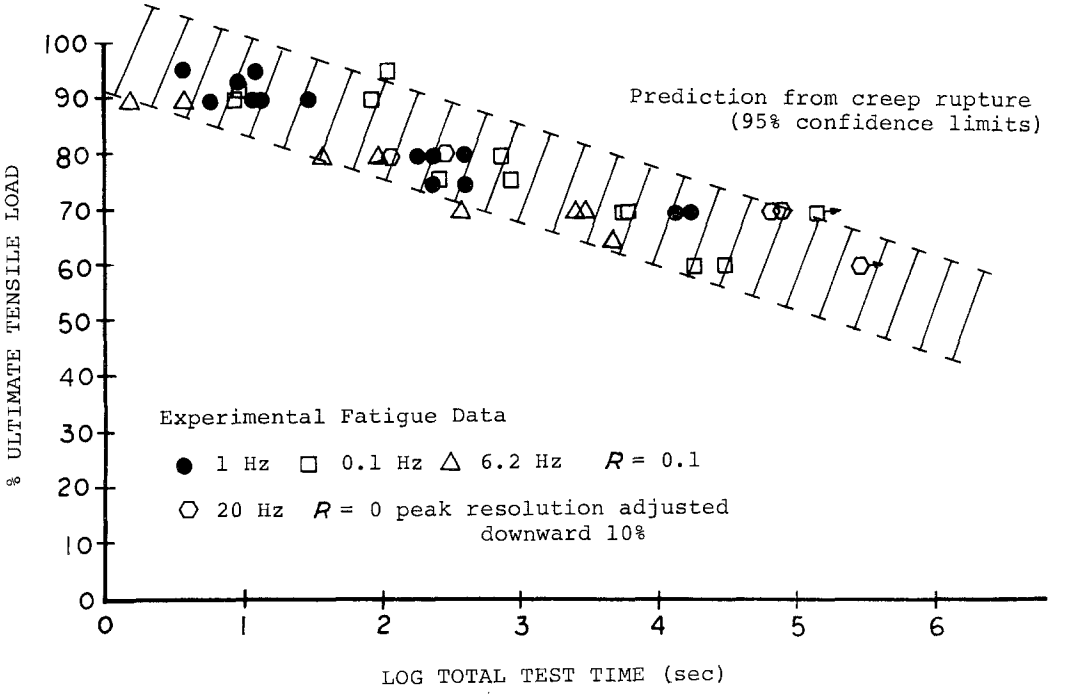

Figure 12 Comparison of single nylon fibre cyclic fatigue data with prediction from creep rupture based model.

$$t_b = \frac{\hat{t}(p)}{I_0(BQ)} \quad (4)$$

where $\hat{t}(p)$ is the time to fail under a constant load equal to the mean load p, B is the slope from Equation 2, and Q is the amplitude from Equation 3. To summarize, creep rupture times are integrated over a varying load to calculate the fatigue failure time.

Calculated failure times based on yarn and fibre creep rupture data are compared to the actual experimental fatigue data points in Figs. 12 and 13. (Confidence limits on the graphs were determined by finding the 95% limits on the creep rupture pre-exponential terms, and then using these bounds for the creep rupture equation in the integration procedure.) Single fibre behaviour is very well predicted by the creep rupture model. This behaviour is common to several other highly oriented fibres which were also examined briefly. Aramid (Kevlar 49) and polyester (DuPont D608 PET) single fibre data, shown in Figs. 14 and 15, both conform to the model.

In contrast, yarn (Fig. 12) does not conform as well; the data consistently fall below the model prediction. Note that different sets of creep rupture data are used in the single fibre and yarn predictions; single fibre creep is used in the single fibre prediction and yarn creep is used in the yarn prediction. Since it has been shown that the single fibres and yarns have the same normalized S–N behaviour under cyclic loading at different frequencies, it is clear that the difference in model accuracy between yarns and single fibres must derive from differences in their creep rupture behaviour. Fig. 16 compares the creep rupture curves for single fibres and yarns. (The ultimate load used to normalize the creep data is determined in a ramp test with a total failure time of approximately 0.5 sec). The yarn creep rupture curve is clearly less steep. A comparison of Figs. 12 and 13 shows that the yarn cyclic fatigue data are predictable from the creep rupture model if the single fibre creep rupture curve is used in the prediction.

The less steep creep rupture slope of the yarn may be explained by the observation that, in a yarn structure under constant dead load, individual broken fibres may be caught within the structure and reloaded along part of their length. In a yarn undergoing cycling, on the other hand, the structure continually opens and closes, allowing broken fibres to work free and become completely unloaded; this is, in fact, visually observed.

The question of relative fibre movement within

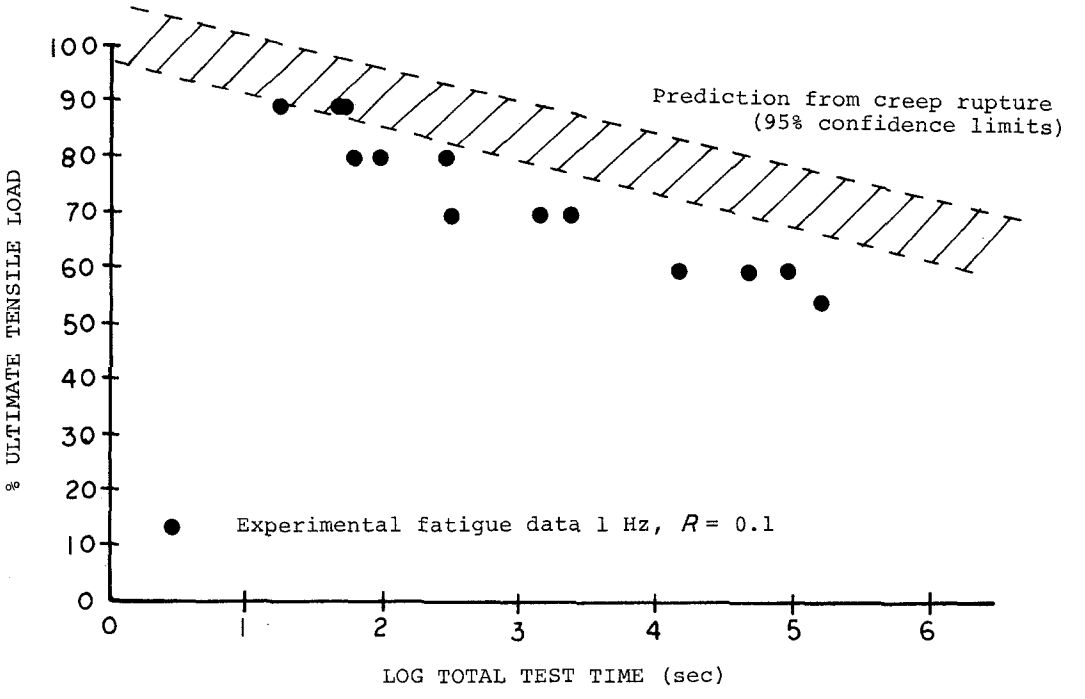

Figure 13 Comparison of nylon yarn cyclic fatigue data with prediction.

the yarn during cycling was examined in a series of yarn fatigues at varying R ratios (0.1, 0.5, and 0.8). Fig. 17 indicates that higher R ratios, resulting in reduced opening and closing of the structure, approach the limit of constant loading or creep rupture at $R = 1$.

A series of experiments was conducted to directly observe the behaviour of yarns containing

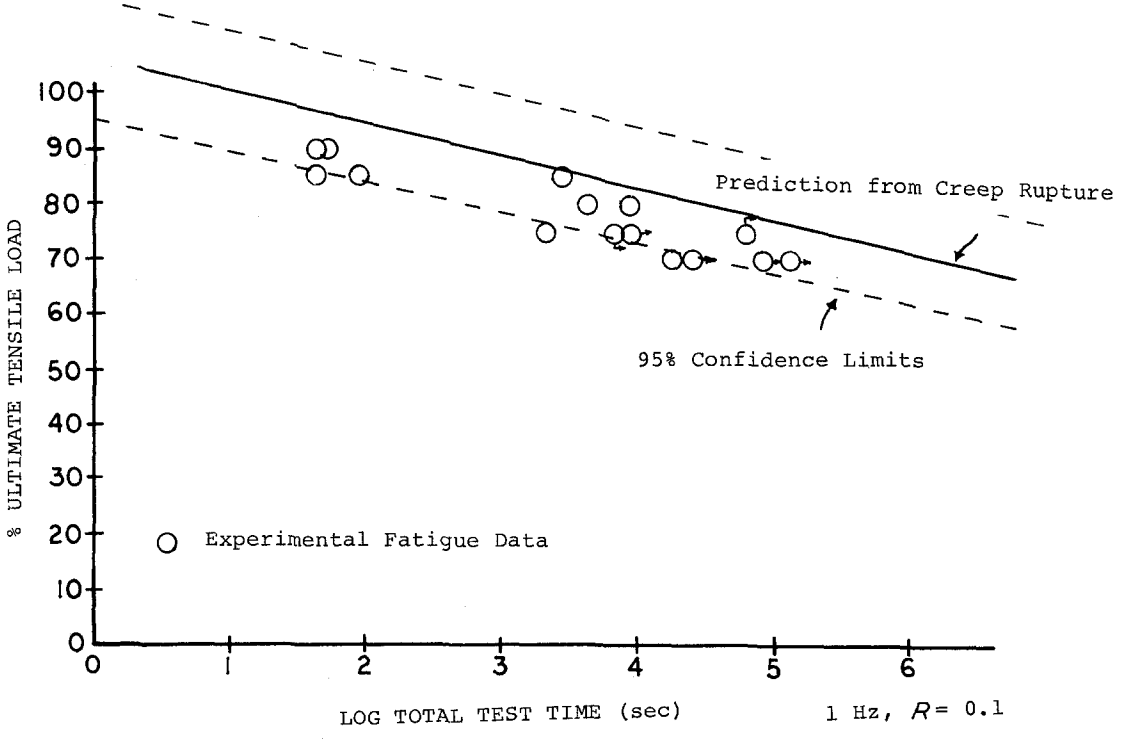

Figure 14 Comparison of single aramid fibre cyclic fatigue data with prediction.

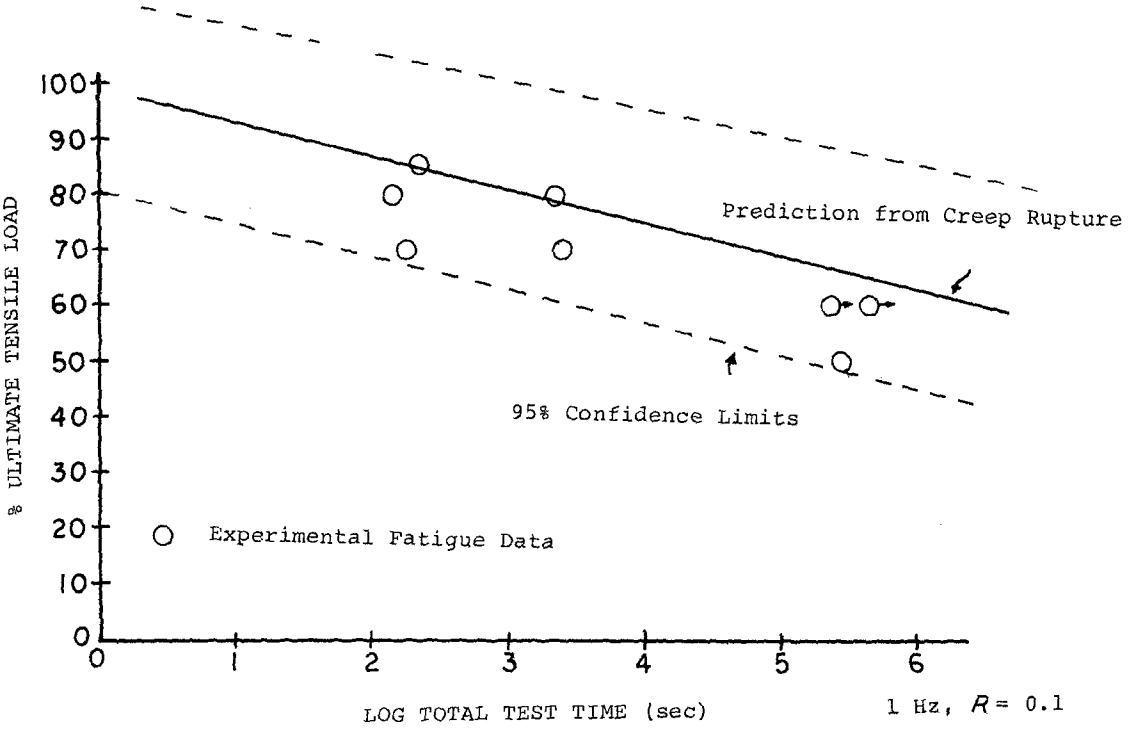

Figure 15 Comparison of single polyester fibre cyclic fatigue data with prediction.

some cut fibres to simulate broken fibres. In these experiments, several fibres within the structure were cut, their ends and starting positions marked, and displacement of the ends examined after 1000 cycles at 70% of ultimate load. From the location of the fibre ends, the amount of strain on the cut fibres, compared to the yarn as a whole, may be calculated. The results given in Table IV show an increasing amount of average strain over the cut fibre length, and corresponding

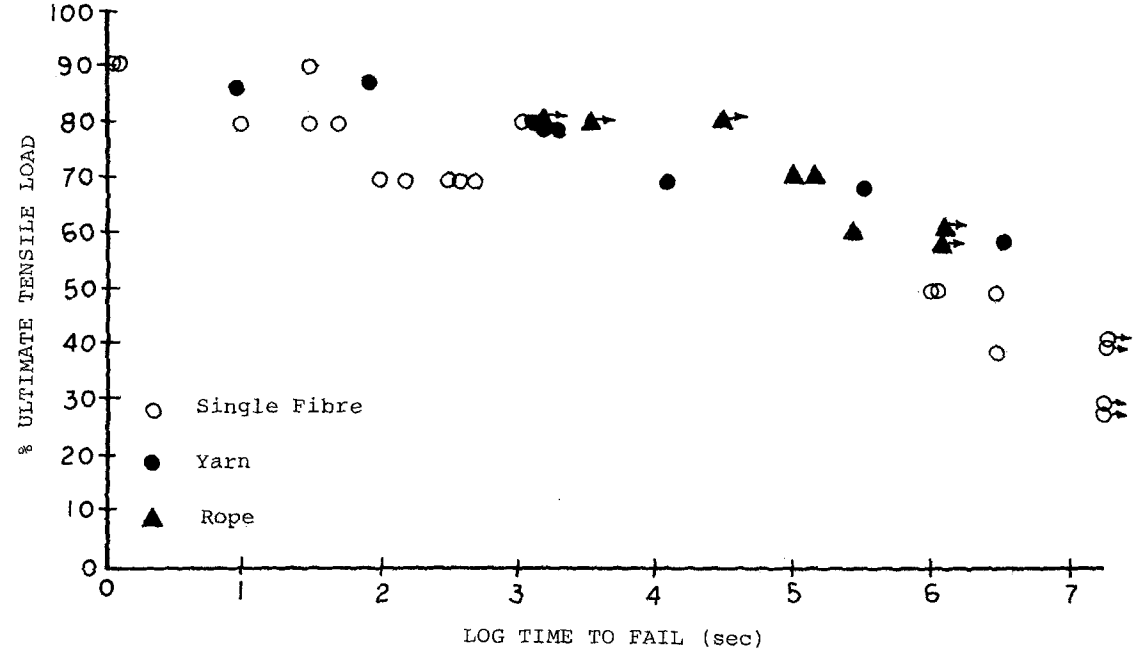

Figure 16 Comparison of creep rupture data for nylon single fibres, yarns and 3/16 in. double braided rope.

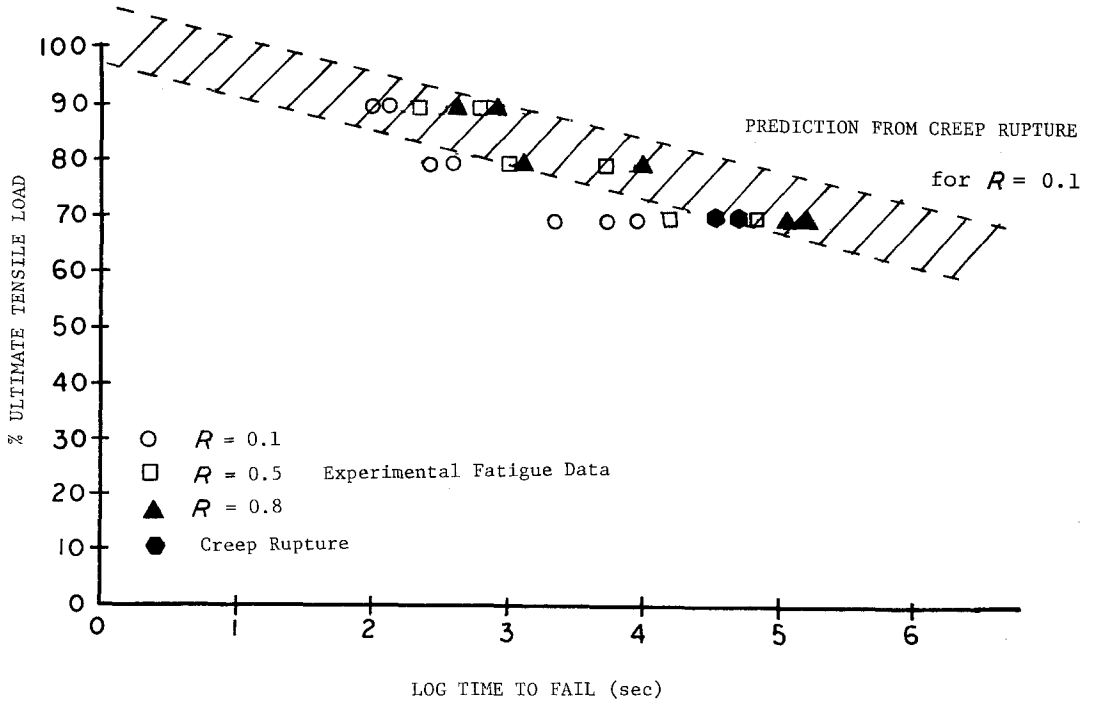

Figure 17 Effect of R ratio on fatigue of nylon yarns.

greater average loading in the cut fibres at higher R ratios, approaching a maximum during creep rupture. Thus, the fibres are only partially unloaded, and the less steep creep rupture curve of yarn may derive from this effect. Cycling at the usual $R = 0.1$ reduces this process, so the fibre and yarn data agree in cyclic fatigue. Similar reloadings may occur in small ropes as well, although the amount will necessarily be affected by the complex geometric structure.

4. Conclusions

The fatigue resistance of nylon single fibres, yarns and small ropes are all nearly identical on normalized S–N scales, at all frequencies tested. Yarns and single fibres fail by a creep rupture mode depending on the total time under load, not the number of cycles. A cumulative time under load, creep rupture model for fibres can accurately predict the failure in cyclic tests at different frequencies. Other oriented fibres (polyester and aramid) also agree with this creep rupture model. Consistent with a creep rupture dominated mode, the strain at failure for a given structure is independent of the type of loading, including ramp (tensile test), creep rupture, or cyclic fatigue. The model is less accurate for yarns, as the baseline creep rupture curves become less steep in going from fibre to yarn. This may arise from broken fibres which are partially reloaded in the higher levels of structure. However, the yarn cyclic data are accurately predicted when the single fibre creep rupture data are used in the model prediction.

TABLE IV Analysis of fibre movement in yarn after 1000 cycles at 70% ultimate load, 1 Hz

R ratio	Number of cut fibres	Average % strain along cut fibre length
0.1	9	0
0.5	3	1.5
	6	0
0.8	4	5.4
	6	3.1
1.0	5	7.9
	5	4.7

Acknowledgement

This research is part of a broad study of the deterioration of synthetic marine rope supported by the Naval Sea Systems Command through the MIT Sea Grant Program. Mr George Prentice is the Navy's technical liaison person on the project.

References

1. N. STARSMORE, M. G. HALLIDAY and W. A. EWERE, "Barge Motions and Towline Tensions

Measured During a North Sea Tow", in Proceedings of the International Symposium on Ocean Engr. – Ship Handling, Gothenberg, Sweden (1980) paper 13.
2. R. W. HERTZBERG and J. A. MANSON, "Fatigue of Engineering Plastics" (Academic Press, New York, 1980).
3. J. A. MANSON and R. W. HERTZBERG, *CRC Crit. Rev. Macromol. Sci.* **1** (1973) 433.
4. G. B. McKENNA and R. W. PENN, *Polymer* **21** (1980) 213.
5. B. D. COLEMAN, *J. Polym. Sci.* **20** (1956) 447.
6. A. R. BUNSELL and J. W. S. HEARLE, *J. Appl. Polym. Sci.* **18** (1974) 267.
7. R. L. HAMILTON and C. H. MILLER Jr, *Textile Res. J.* **34** (1964) 20.
8. J. W. S. HEARLE, *J. Mater. Sci.* **2** (1967) 474.
9. I. NARISAWA, M. ISKIKAWA and H. OGAWA, *J. Polym. Sci.* **15** (1977) 1055.
10. A. R. BUNSELL and J. W. S. HEARLE, *J. Appl. Polym. Sci.* **18** (1974) 267.
11. W. T. KELLEY, *Textile Res. J.* **35** (1965) 852.
12. M. M. PLATT, W. G. KLEIN and W. J. HAMBURGER, *ibid.* **22** (1952) 641.
13. W. J. LYONS, *ibid.* **32** (1962) 553.
14. A. PETERLIN, *J. Polym. Sci.* **7A–2** (1969) 1151.
15. D. C. PREVORSEK, P. J. HARGET, R. K. SHARMA and A. C. REIMSCHUESSEL, *J. Macromol. Sci. Phys.* **1–2B8** (1973) 127.
16. J. W. S. HEARLE and E. A. VAUGHN, *Rheol. Acta* **9** (1970).
17. A. R. BUNSELL and J. W. S. HEARLE, *ibid.* **13** (1974) 711.

Received 24 May
and accepted 19 July 1984